3D3-2

POLSAR Image Analysis for Wetlands Monitoring Based on a Modified Four-component Scattering Power Decomposition

Yuki Yajima [1], [#] Ryoichi Sato [2], Yoshio Yamaguchi [3],
Hiroyoshi Yamada [3] and Wolfgang-Martin Boerner [4]

[1] Graduate School of Science and Technology, Niigata University, Japan
[2] Faculty of Education and Human Sciences, Niigata University
8050, 2-no-cho, Ikarashi, Niigata, 950-2181 Japan
E-mail: sator@ed.niigata-u.ac.jp
[3] Department of Information Engineering, Niigata University, Japan
[4] Department of Electrical and Computer Engineering, University of Illinois at Chicago, USA

1. Introduction

Monitoring or observation of natural resources is one of the most important applications of Polarimetric Synthetic Aperture Radar (POLSAR) sensing. Decomposition of polarimetric scattering matrices acquired by POLSAR system can provide the contribution of scattering mechanism and tell us the change of environmental issue by comparing data sets of continuous observations [1]- [4]. A four-component scattering power decomposition method [3], [4] is one of the most effective classification techniques. In the decomposition scheme, total scattering contribution is decomposed into four scattering mechanisms as surface scattering, double-bounce scattering, volume scattering and helix scattering. In particular, the scheme based on the coherency matrix [4] is more suitable for direct physical interpretation of data and phenomena, easy calculation and implementation. However, there exists a drawback such that some negative power components are observed in the image analysis although the occurrence is not frequent. The negative power is inconsistent with physical condition.

In this paper, to overcome the problem, we introduce a modification for the decomposition procedure by making all the decomposed powers be positive from the physical point of view. Namely, we modify the decomposition scheme by the power restriction that all the decomposed powers should be greater than 0 and less than the total power. To confirm the validity of the modification, some image analyses are carried out for high resolution POLSAR data. Here, a small lagoon "Sakata" and the surrounding wetland, located in Niigata Prefecture, Japan, are chosen as the site for the analyses. Seasonal environmental change of the wetland area is also investigated by the image analyses.

2. Four-component Power Decomposition

First, let us briefly show the decomposed procedure for the coherency matrix $[T]$, whose components are obtained by elements of Sinclair scattering matrix as

$$[S(HV)] = \begin{bmatrix} S_{HH} & S_{HV} \\ S_{VH} & S_{VV} \end{bmatrix} = \begin{bmatrix} a & c \\ c & b \end{bmatrix}, \tag{1}$$

where $S_{HV} = S_{VH} = c$ for back scattering case. The average coherency matrix $\langle[T]\rangle$ is given as

$$\langle[T]\rangle = \frac{1}{2}\begin{bmatrix} \langle|a+b|^2\rangle & \langle(a+b)(a-b)^*\rangle & \langle 2(a+b)c^*\rangle \\ \langle(a-b)(a+b)^*\rangle & \langle|a-b|^2\rangle & \langle 2(a-b)c^*\rangle \\ \langle 2c(a+b)^*\rangle & \langle 2c(a-b)*\rangle & \langle 4|c|^2\rangle \end{bmatrix}, \tag{2}$$

where $\langle\cdot\rangle$ denotes the ensemble average in the data processing. The measured coherency matrix $\langle[T]\rangle$ can be expanded into four components as

$$\langle[T]\rangle = f_s\langle[T]\rangle_{surface} + f_d\langle[T]\rangle_{double} + f_v\langle[T]\rangle_{vol} + f_c\langle[T]\rangle_{Helix}, \tag{3}$$

ISBN: 978-4-88552-223-9 C3055

where $\langle[T]\rangle_{surface}$, $\langle[T]\rangle_{double}$, $\langle[T]\rangle_{vol}$ and $\langle[T]\rangle_{Helix}$ are the coherency matrices for surface scattering, double-bounce scattering, volume scattering and Helix scattering, respectively. Also, f_s, f_d, f_v, f_c are the unknown deterministic coefficients for each scattering component.

For the surface and double-bounce scattering models, the corresponding matrices are expressed as

$$[T]_{surface} = \begin{bmatrix} 1 & \beta^* & 0 \\ \beta & |\beta|^2 & 0 \\ 0 & 0 & 0 \end{bmatrix}, \quad |\beta| < 1, \qquad [T]_{double} = \begin{bmatrix} |\alpha|^2 & \alpha & 0 \\ \alpha^* & 1 & 0 \\ 0 & 0 & 0 \end{bmatrix}, \quad |\alpha| < 1, \tag{4}$$

where α and β are unknowns to be determined. While, for the volume scattering model, we choose one of the following average matrices according to the ratio of the co-polarized components, *i.e.* $CoPol = 10\log_{10}(\langle|S_{HH}|^2\rangle/\langle|S_{VV}|^2\rangle)$. For $CoPol$ >2dB, $|CoPol|$ <2dB, and $CoPol$ < −2dB, we can choose $\langle[T]\rangle_{vol}$ as

$$\langle[T]\rangle_{vol} = \frac{1}{30}\begin{bmatrix} 15 & 5 & 0 \\ 5 & 7 & 0 \\ 0 & 0 & 8 \end{bmatrix}, \quad \langle[T]\rangle_{vol} = \frac{1}{4}\begin{bmatrix} 2 & 0 & 0 \\ 0 & 1 & 0 \\ 0 & 0 & 1 \end{bmatrix}, \quad and \quad \langle[T]\rangle_{vol} = \frac{1}{30}\begin{bmatrix} 15 & -5 & 0 \\ -5 & 7 & 0 \\ 0 & 0 & 8 \end{bmatrix}, \tag{5}$$

respectively. The matrix for Helix scattering model is

$$\langle[T]\rangle_{helix} = \frac{1}{2}\begin{bmatrix} 0 & 0 & 0 \\ 0 & 1 & \pm j \\ 0 & \mp j & 1 \end{bmatrix}. \tag{6}$$

Substituting the measured data into the left-hand side $\langle[T]\rangle$ of Eq.(3), and making comparisons between the matrix elements for the both sides, one can obtain the unknowns f_s, f_d, f_v, f_c. Resultantly, the decomposed four scattering powers P_s, P_d, P_v, P_c can be derived.

3. Modification of the decomposition algorithm

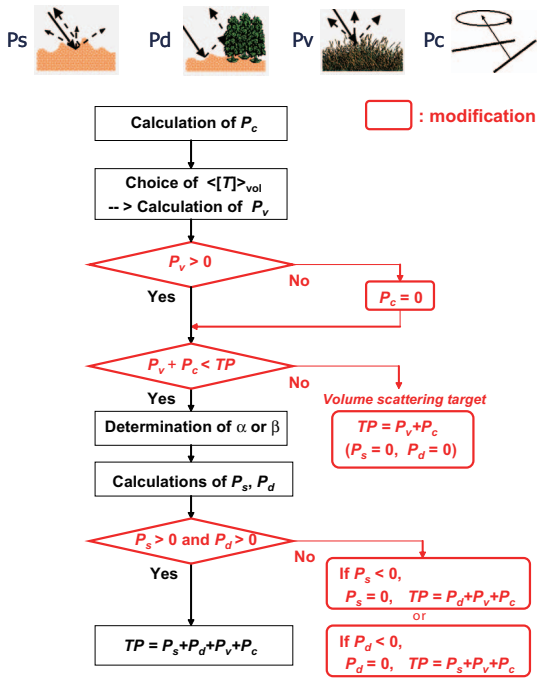

Figure 1: A modified four-component decomposition algorithm

Figure 1 shows the modified algorithm for the four-component scattering power decomposition. The present modification is based on the power restriction that all the decomposed powers should be greater than 0 and less than the total power. As can be seen in the next section, this power restriction yields more accurate and acceptable results.

4. Rusults of POLSAR image analysis

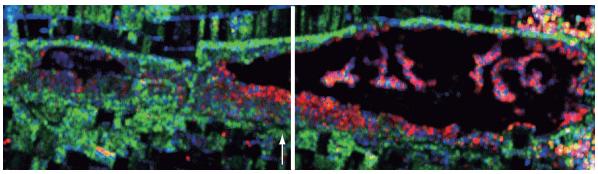

(a) Color composite image, Aug. 2004

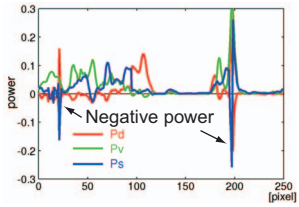

(b) Without modification

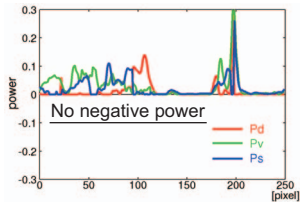

(c) With modification

Figure 2: L-band decomposed image

We applied the modified scheme to high resolution data sets acquired with Pi-SAR over a lagoon "Sakata" and the surrounding wetland. Pi-SAR is an airborne polarimetric SAR system developed by NiCT and JAXA, Japan. It has dual frequency (L- and X-) bands. The resolution on the ground is 2.5 by 2.5 m in the L band and 1.25 by 1.25 m in the X band.

Let us first check the validity of the present modification for the power decomposition method. Figure 2 shows the decomposed result of L-band image data in mid-summer season. Fig.2 (a) is the color composite image. In the figure, the scattering powers are color-coded as Green for P_v (volume scattering), Red for P_d (double bounce scattering), and Blue for P_s (surface scattering). Since P_c was small enough compared to other powers, it was omitted here to illustrate. Fig.2 (b) and (c) are the decomposed results along a transect across the lagoon (See Fig.2 (a)) with and without the modification, respectively. It is seen from the figures that the negative powers which look like spiky noise completely diminish and the modified decomposition result (c) seems quite natural. The strong double-bounce scatterings can also be observed at the boundaries between the water area and the surrounding emerged-plant areas. The contribution of the strong P_d may be utilized for monitoring the status of bushes, reeds, lotus around the wetland [5]. For winter and autumn seasons of Fig.3 (a) and (b), the double-bounce scattering P_d is still observed, although the brightness of the Red color is small.

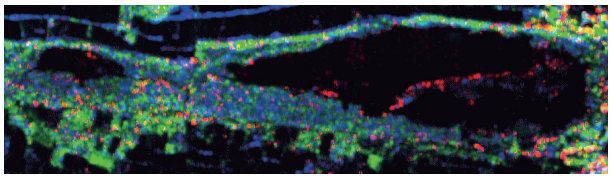

(a) Color composite image, Feb.2004

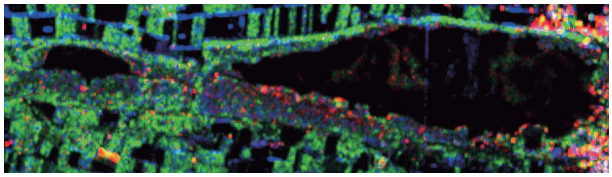

(b) Color composite image, Nov.2004

Figure 3: L-band decomposed images

While, in the X-band images of Fig.4, due to the difference of the scattering mechanism in frequency, Green (P_v) and/or Blue (P_s) color becomes dominant within the emerged-plants around the lagoon, instead of Red color (P_d). Since the X-band waves cannot deeply penetrate into the vegetation, most of the X-band scattering waves may be generated at the upper or middle parts of the plants. So the vegetation may no longer act as corner reflector.

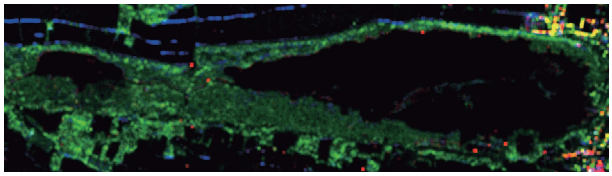

(a) Color composite image, Feb.2004

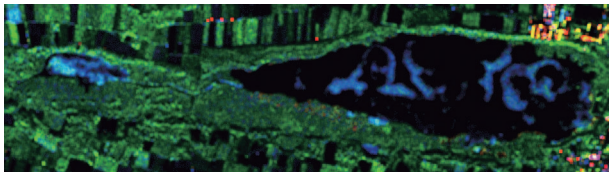

(b) Color composite image, Aug.2004

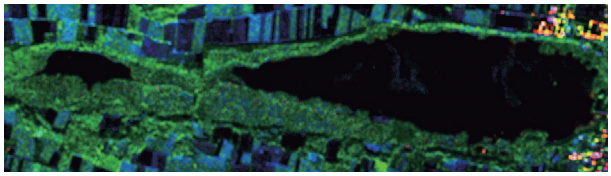

(c) Color composite image, Nov.2004

Figure 4: X-band decomposed images

Acknowledgments

The authors express their sincere appreciations to NiCT and JAXA, Japan, for providing valuable Pi-SAR image data. This research was partially supported by a Scientific Research Grant-In-Aid from JSPS, Japan.

References

[1] H. Mott, "Remote sensing with polarimetric radar," IEEE Press, 2007.

[2] A. Freeman and S. L. Durden, "A Three-component scattering model for polarimetric SAR data," *IEEE Trans. Geosi. Remote Sensing*, Vol.36, No.3, pp.963-973, May 1998.

[3] Y.Yamaguchi, T.Moriyama, M.Ishido, and H.Yamada, "Four-Component Scattering Model for Polarimetric SAR Image Decomposition," *IEEE Trans. Geosci. Remote Sensing*, vol.43, No.8, pp.1699-1706, Aug. 2005.

[4] Y. Yamaguchi, Y.Yajima, H.Yamada, "A Four-Component Decomposition of POLSAR Images Based on the Coherency Matrix," *IEEE Geosci. Remote Sensing Letters*, vol.3, No.3, pp.292-296,July 2006.

[5] R. Sato, Y. Yajima, Y. Yamaguchi, and H. Yamada, "Investigation on Seasonal Water Area Change in Lake Sakata Based on POLSAR Image Analysis," submitted to *IEICE Trans. on Commun.*.